CH/Tech/98/01

PSD Signal Timing

A reminder and overview

Author: R.L. Cowin

Date: March 2, 1998

Timing Aspects of Sheet–Resistor PSDs

PREAMBLE

Recently (January 1998), and for the first time, the sheet resistor type of position–sensitive detector[1] (PSD) was used in the MEGHA strip array and hooked–up to the new data acquisition (DA) without much success. Previously these detectors have been used in the MEGHA telescope modules and instrumented using a variety of different configurations of the 'old' CHARISSA DA, each time with limited success.

It is becoming apparent that every time they are used they exhibit different characteristics and (a variety of) faults/problems (particularly high energy thresholds). This indicates that the problem lies with the methods used to instrument these detectors, and the exact DA configuration. This is confirmed by simple α–particle tests using the 'self–gating' GLADYS [1] DA system which requires no logic discrimination or signal coincidences for operation. Energy thresholds in this case have been measured as low as 1→2MeV.

The ultimate culprit for the continued poor performance of this detector type is probably the high (intrinsic) junction capacitance. The high capacitance, coupled with the surface resistance, gives a delay–line effect which slows the charge collection [2] and hence delays the firing of leading edge discriminators within the main amplifier. This results in large time–walk as a function of position [3] and energy [4]. The sophisticated DA systems employed by CHARISSA depend upon rigorous timing constraints, to discriminate valid events from noise and randoms, using fast NIM logic electronics triggering, and are thus highly sensitive to these time–walks. In the past this has led to the rejection of valid events in the DA hardware [3, 4].

[1] All data presented here were obtained from a Hamamatsu 50mm×50mm×385μm PSD

1 Introduction

This report is intended to form an overview of the various aspects of PSD signal timing and how they influence the data acquisition. Although the majority of the data presented here were obtained using the 'old' DA in many cases the effect of the specific DA configuration can be 'deconvolved' to a certain extent from the data. This deconvolution has been helped enormously by use of the PSD model described in reference [2]. Thus the results presented are still valid for the 'new' DA. However the conclusions as to how the new DA will handle the PSD data are still tentative and very much open to further interpretation and discussion.

It is hoped that this document will form the basis of further discussion on this subject. This is particularly important considering both the large financial investment in these detectors and the proximity of the forthcoming experimental period (begins 14^{th} March).

2 Energy Threshold

The low energy detection threshold in a PSD is a complex function of the signal rise–times, the main amplifier (MA) discriminator levels, the MA gain, the ADC conversion thresholds and the logic electronics set–up. This section attempts to quantify the contributions to the measured PSD detection threshold from these sources using the PSD model [2].

Two experiments have been performed with PSDs mounted in the MEGHA modules and instrumented using the old DA. The first experiment, labelled COINC here, required a coincidence within 500ns between the shaped discriminator pulses from the Gas energy signal[2] (ΔE_{Gas}), the PSD energy signal (E_{PSD}) and the *fastest* PSD position signal (a or b or c or d). A schematic of the COINC analogue and logic electronics is shown in figure 1. The second experiment is described in section 3.

2.1 Experimental Set–up

Old style CHARISSA MAs were used to shape the PSD position signals (and the Gas and CsI–PD energy signals) with a shaping time constant of $1.5\mu s$. The PSD energy signals were shaped by ORTEC 572 spectroscopy amplifiers using a time constant of $6\mu s$. Each bipolar MA output was then passed to a SILENA 4418/V ADC without further processing. For the PSD energy signals the discriminator pulses were obtained by feeding the PA output to both an ORTEC and CHARISSA MA. The discriminator

[2] For the data presented here the gas ionisation chamber was not filled with propane and so the Gas energy signal coincidence requirement was removed

pulses from the CHARISSA MAs were then shaped and input to the coincidence unit.

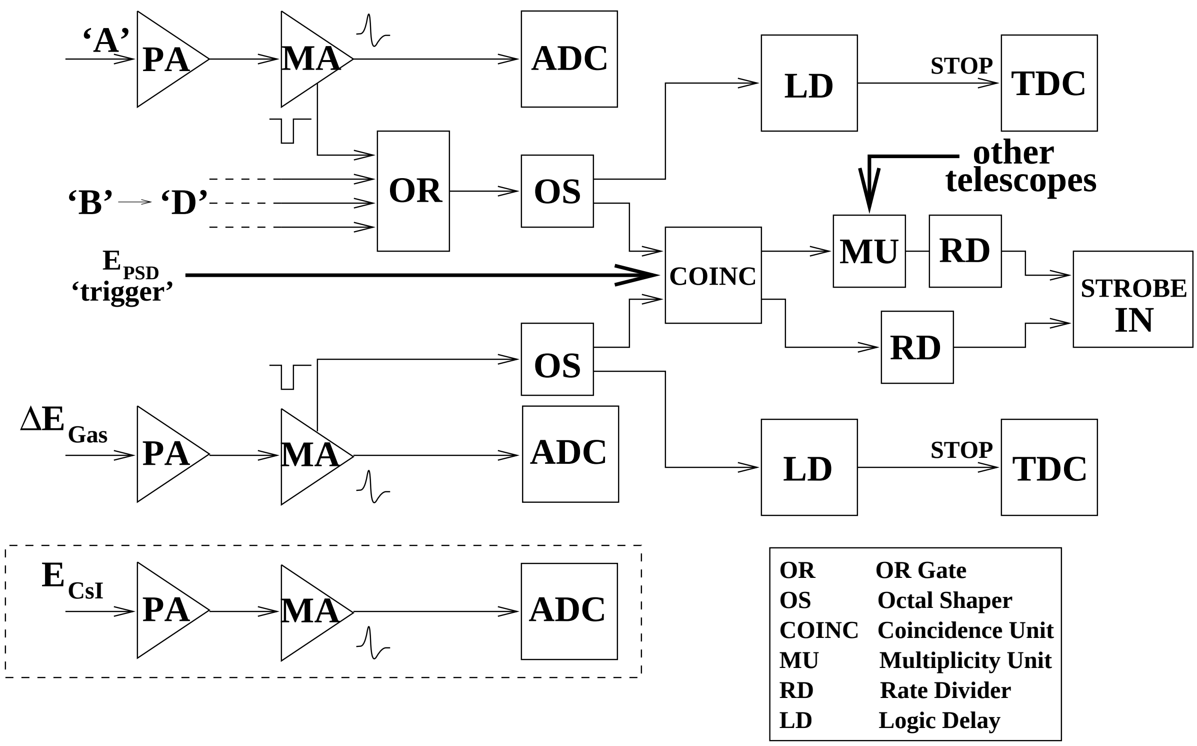

Figure 1: Schematic of the COINC analogue and logic electronics.

2.2 Results

In order to completely reconstruct the energy and position of a particle hit within a PSD, the five signals had to fulfill three criteria;

1. To be recorded in their respective ADCs, the signals had to be large enough to surpass the ADC conversion threshold (V_{ADC}), that is,

$$E_{PSD},\ A,\ B,\ C \text{ and } D\ >\ E_{ADC} \tag{1}$$

   where E_{ADC} is the energy equivalent of V_{ADC}. Bruno *et al.* [5] noted that the four position signals are proportional to the energy deposited in the PSD, viz,

$$\begin{aligned} A &= E_{PSD}\ .\ f(X,Y) \\ B &= E_{PSD}\ .\ g(X,Y) \\ C &= E_{PSD}\ .\ h(X,Y) \\ D &= E_{PSD}\ .\ l(X,Y) \end{aligned} \tag{2}$$

and that, from conservation of electric charge,

$$f(X,Y) + g(X,Y) + h(X,Y) + l(X,Y) = 1 \tag{3}$$

and from the symmetry properties of the PSD,

$$f(0,0) = g(0,0) = h(0,0) = l(0,0) = 0.25 \tag{4}$$

(where (X,Y)= (0,0) is the PSD centre). From equations 2 and 1 the minimum energy (E^{ADC}_{thresh}) which must be deposited in the PSD to fulfill criteria 1. is seen to be,

$$E^{ADC}_{thresh} = \frac{E_{ADC}}{f(X,Y)}\text{ , or }\frac{E_{ADC}}{g(X,Y)}\text{ , or }\frac{E_{ADC}}{h(X,Y)}\text{ , or }\frac{E_{ADC}}{l(X,Y)} \tag{5}$$

whichever is the largest. The value of E_{ADC} was not measured in the COINC experiment and has therefore been regarded in this analysis as a legitimate degree–of–freedom in fitting the model prediction to the experimental data. The PSD model was used to calculate the values of f, g, h and l and hence E^{ADC}_{thresh}. The results for E_{ADC}= 2.3MeV are plotted in figure 2. The minimum threshold of 9.2MeV is simply given by $4\times E_{ADC}$ and occurs at the PSD centre. The threshold at the centre of each edge is 15.8MeV, and the maximum threshold of 22.4MeV is at each of the four corners. It is immediately apparent that the minimum threshold for a PSD is likely to be at least twice as high as that for a strip detector (PSSD) since a PSSD requires only two position signals above ADC threshold. The high junction capacitance of a large area PSD as compared to a PSSD also leads to a larger noise level, requiring higher ADC and amplifier discriminator thresholds and leading to a still higher energy detection threshold.

2. The logic electronics required that one of the four position signals surpassed its MA discriminator level to generate a NIM logic pulse, and that,

3. this position–signal–derived NIM pulse arrived at the coincidence unit (figure 1) within 500ns of the corresponding energy–signal–derived NIM pulse, to fulfill the coincidence requirement. The PSD model was also used to examine the effects of criteria 2. and 3. on the energy threshold.

Figure 3(a) shows a plot of the time difference (t_{ep}) between the generation of the fastest position NIM pulse and the corresponding energy NIM pulse as a function of E_{PSD} for several positions of particle incidence, calculated using the PSD model. The data were obtained by calculating the time taken for both the

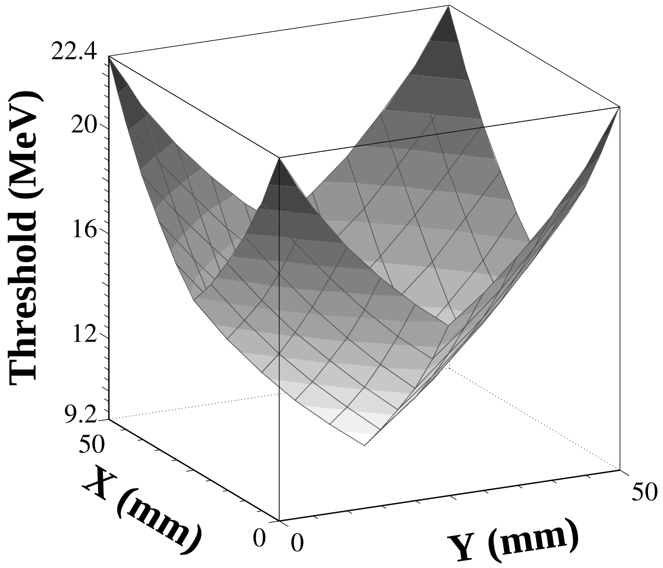

Figure 2: Calculated ADC–induced energy threshold (E_{thresh}^{ADC}) in the PSD as a function of the position co–ordinate.

energy and position signals to rise above an arbitrary voltage level (V_{disc}^{M}), to mimic the MA discriminator level, as a function of the magnitude [energy] of the initial condition (equation [2.12] in reference [2]). Positive values of t_{ep} indicate that the position NIM pulse is slower than the energy NIM pulse. It can be seen that the value of t_{ep} is energy and position dependent, and is greatest for low energy events at the PSD centre.

For a coincidence overlap t_{ep} must be less than 500ns. Equivalently, it can be seen that a minimum energy must be deposited in the PSD, and that this energy threshold, E_{thresh}^{COINC}, is position dependent. Since the MA discriminator levels were not measured, the model energy–scale was calibrated by varying V_{disc}^{M} to match the model prediction of E_{thresh}^{COINC} to the experimental data. This gave a reasonable estimation of the energy equivalent of the MA discriminator level, E_{disc}, of 3.5MeV.

The values of E_{thresh}^{ADC} and E_{thresh}^{COINC} are compared, in figure 4, to the low energy detection threshold of the PSD. It can be seen that the energy threshold near the edges of the PSD is given by the ADC induced threshold (dashed line) and that near the detector centre the high energy threshold is due to the fact that the position and energy NIM pulses arrive at the coincidence unit separated by 500ns or more (t_{ep} >500ns below the dotted line).

The energy threshold is thus seen to be very sensitive to the timing requirements, and also unacceptably large for a 500ns wide energy AND fastest–position coincidence requirement. From figure 3(a) it can be seen that at low energy the timing quickly

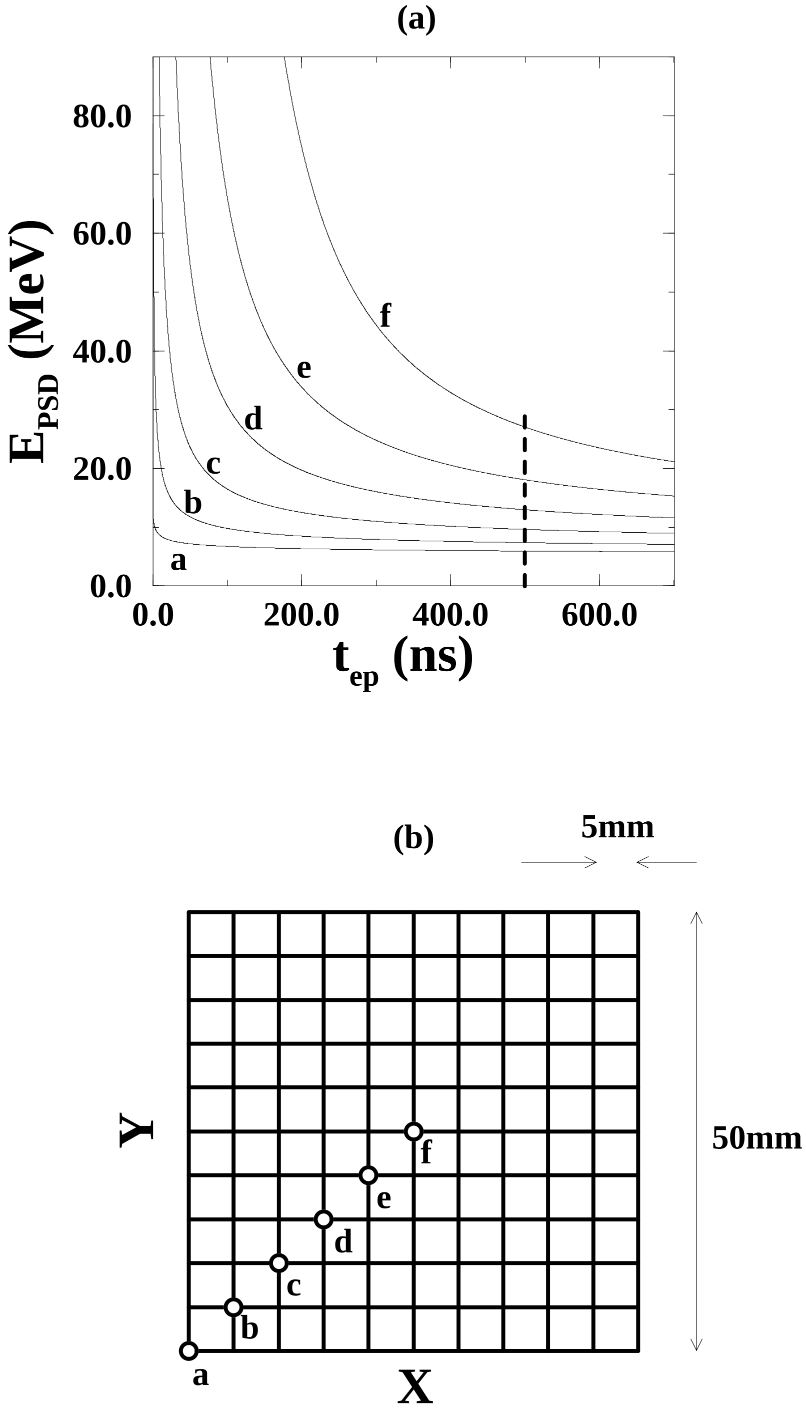

Figure 3: (a) Time difference between PSD energy and position signal timing as a function of particle energy, for a MA discriminator level (E_{disc}) of 3.5MeV. (b) Schematic of the PSD model nodal mesh to illustrate the simulated positions of incidence used to generate the data in (a).

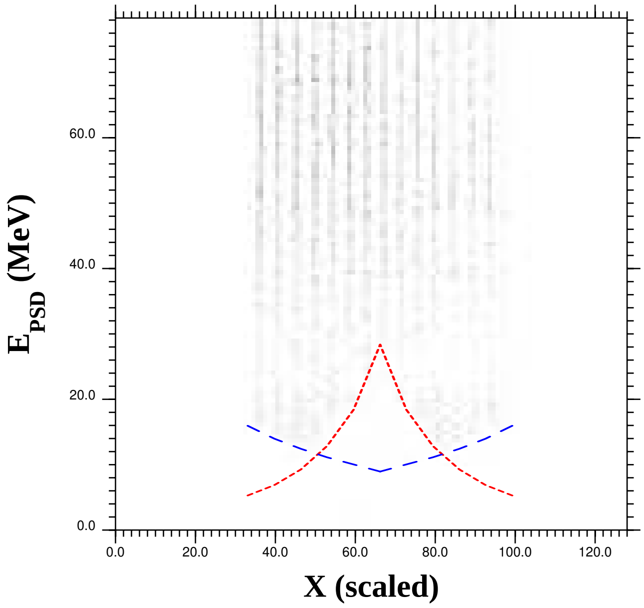

Figure 4: Plot of E_{PSD} against X for a central 2mm wide slice of data across the face of the PSD. The dashed and dotted lines highlight the calculated variations in E^{ADC}_{thresh} and E^{COINC}_{thresh} respectively.

becomes very poor, so that a widening of the coincidence overlap leads to only a small reduction in the energy threshold.

3 PSD Signal Timing

The logic electronics for the second experiment, labelled LOOSE, were arranged so that TDC data were recorded for all signals. Also, to simplify the trigger requirement to enable an unconstrained ('LOOSE') investigation of the detector signal timing characteristics, the coincidence units from the COINC experiment were removed from the logic electronics. The minimum trigger requirement possible was to allow the DA to be enabled by the first or only detector signal to rise above the discriminator level set in its MA. [Problems of noise triggering the DA are obvious].

New computer controlled MEGHA MAs were used to shape all detector energy signals, with shaping times[3] of 10μs for the Gas and PSD energy signals, and 2μs for the CsI–PD energy and PSD position signals. Each bipolar MA output was then fed to a SILENA 4418/V ADC without further processing.

The OS outputs for each signal type were passed to an OR gate. The first detector

[3]The MEGHA MA shaping times of 2μs and 10μs are roughly equivalent to ORTEC 572 shaping times of 1.5μs and 5μs respectively.

NIM pulse to arrive propagated first to the STROBE IN gate to trigger the DA. Once the DA was enabled, any further STROBE IN signals generated by slower detector signals were inhibited.

The time taken for a NIM pulse to propagate through the electronics to generate the TDC COMMON START signal was measured to be $\sim$ 180ns. Therefore, the difference between the COMMON START and the $\sim$ 750ns delayed TDC STOP gave a TDC value of $\sim$ 570ns, the 'self–timing' point, for the channel which enabled the data acquisition. All subsequent signals generated a TDC value greater than 570ns. The largest TDC value possible was $\sim$ 1700ns, and was limited by the length of the TDC WINDOW.

3.1 Results

The TDC spectrum for the PSD energy signal is shown in figure 5(a). These data[4] were obtained with no propane in the Gas detector. It can be seen that all events fall within 1ns of the self–timing point, which is indicated by the arrow in the figure. This indicates that the PSD energy signal is always first to rise above its MA discriminator level, viz,

$$t_{disc}(E_{PSD}) \begin{array}{l} < t_{disc}(p) \\ < t_{disc}(E_{CsI}) \end{array} \tag{6}$$

where $t_{disc}(E_{PSD})$, $t_{disc}(p)$ and $t_{disc}(E_{CsI})$ are the times taken for the PSD energy and position and CsI energy signals to rise above their MA discriminator levels respectively.

A spectrum showing the time difference between the PSD energy and fastest position TDC values, which is equivalent to t_{ep}, is plotted in figure 5(b). Also, in figure 5(c), t_{ep} is plotted as a function of the X position co–ordinate for a 2mm wide slice of data across the PSD face extending from corner A to corner C. It can be seen that the position–derived NIM pulses are slower than the corresponding energy–derived NIM pulses by between 10ns at the PSD corners and up to 200ns at the PSD centre. The equivalent PSD model calculation of t_{ep} is plotted as the dashed line in figure 5(c) for comparison.

In the new DA the 800ns duration WALK signals (derived from the leading edge discriminator pulses) are combined in LeCroy 4532 multiplicity modules (MALU) to provide a first level trigger. This defines a global 800ns coincidence requirement which must be met by all signals needed in the second level trigger. Other channels not required by the trigger must produce a WALK signal within 1.6μs of the 'start–

[4] All data from the LOOSE experiment are from $\sim$ 85MeV ^{12}C ions elastically scattered from a ^{197}Au target.

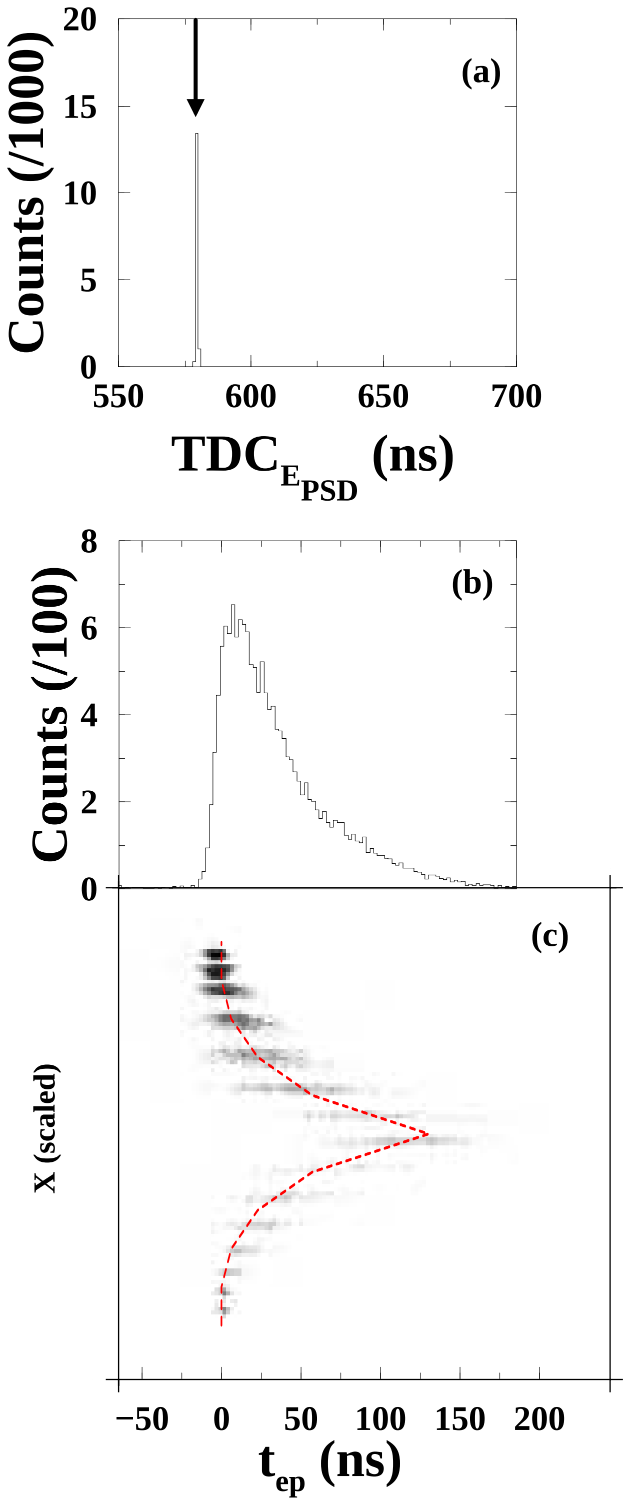

Figure 5: (a) TDC spectrum for the energy signal from the PSD, (b) time difference between the PSD position and energy TDC values and (c) the data in (b) as a function of X for a 2mm wide slice of data across the PSD face.

event–pulse'. Beyond this time all further discriminator pulses are blocked by a BUSY signal.

If the PSD energy and at least one position pulse are required in the first level trigger then the PSD model can be used to predict the energy trend of figure 5(c) and thus the energy below which events at the PSD centre would no longer generate an overlap in the MALU. This is calculated to occur for events depositing less than $\sim$ 14MeV, and give a similar trend with position to the dotted line in figure 4.

Perhaps more interesting is the time–walk of the slower position signals and the gas signals. Figure 6 shows the time difference (t_{eb}) between the PSD energy NIM pulse and 'b' position NIM pulse for a 2mm wide slice of data across the PSD face from corner electrode 'b' to the diagonally opposite electrode. At electrode 'b' (low values of X) the two signal types are in coincidence, but further along the diagonal the position signal begins to lag far behind the energy signal. The upward kink at larger values of X is due to the effects of the low resistance ring electrode configuration – charge flows preferentially around the detector perimeter (see figure 10. in reference [2]).

The equivalent of imposing a 1.6μs limit on the firing of discriminator pulses from a 15MeV event in the PSD can be achieved by requiring in software a 280ns limit on the 85MeV events in this data set[5]. The effect on the XY position spectrum of this requirement is shown in figure 6(b) – 'holes' appear where the position signals are slowest.

A potentially worse problem than mismatches between the PSD energy and position timing is that between the Gas energy and PSD position timing. Whereas both the PSD energy and position signals show a distinct slowing towards the PSD (telescope) centre the Gas signals do not[6]. This exacerbates the problems associated with the requirement that all discriminator signals occur within 1.6μs of the event start.

The time difference between the generation of the fastest PSD position NIM pulse and the Gas NIM pulse (t_{gp}) was measured from the difference in the corresponding TDC values,

$$t_{gp} \quad = \quad TDC_{Gas} - TDC_{position}$$

[5]This assumes that the time to fire a discriminator pulse varies inversely proportional to the pulse height input to the MA. This is true for a preamplifier pulse whose leading edge can be described by a quadratic.

[6]In order to determine whether the Gas TDC signal provided a suitable timing reference point with which to measure the expected variations in $t_{disc}(p)$, the energy dependence of $t_{disc}(\Delta E_{Gas})$ was ascertained. By gating on a small region of the PSD (X,Y) spectrum and also a limited range of E_{PSD}, the variation in t_{gp} could be determined as a function of ΔE_{Gas} only. In this manner, the value of t_{gp} was measured to be independent of the energy deposited in the Gas detector above ΔE_{Gas} =5MeV.

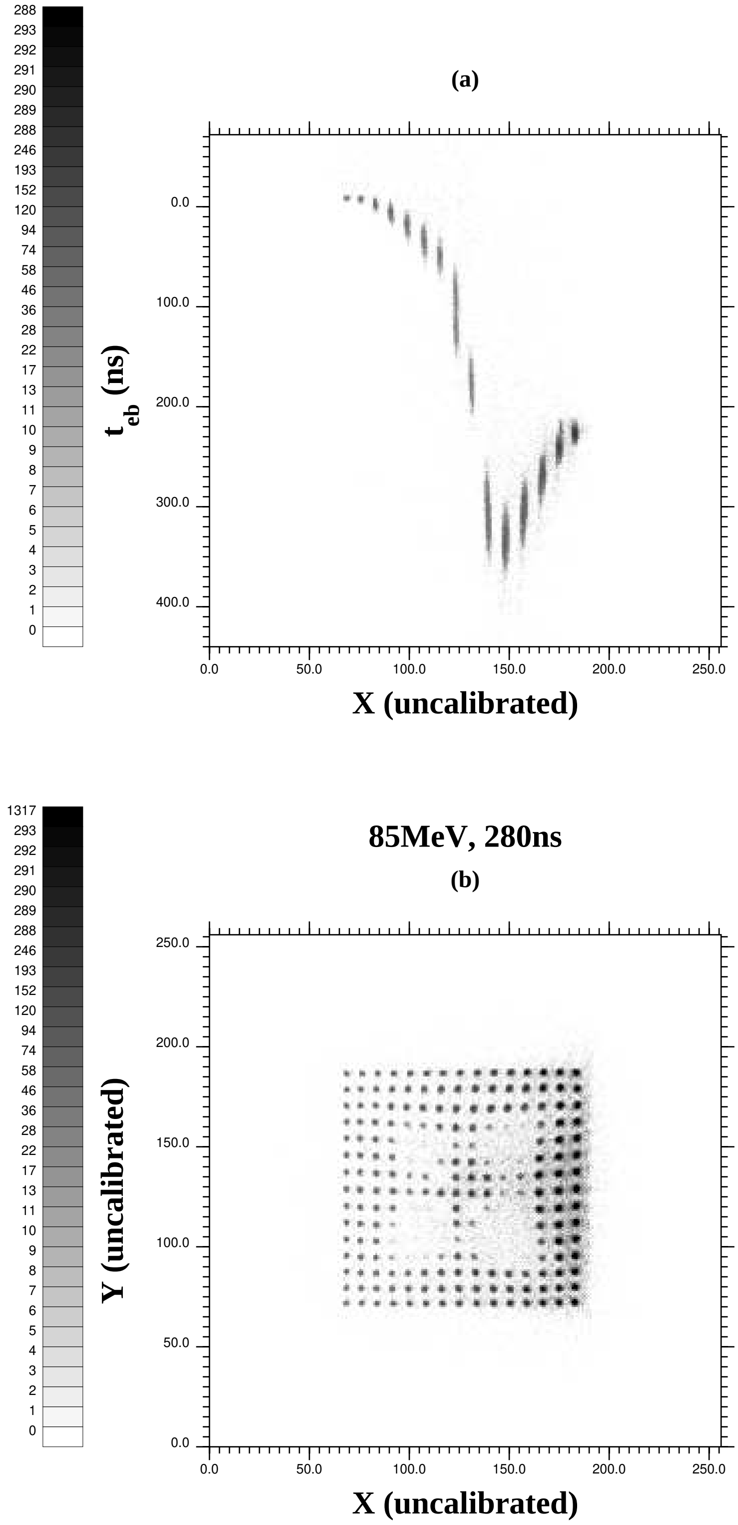

Figure 6: (a) Time difference between PSD energy signal and PSD position signal ‘b’ for a 2mm wide slice of data across the PSD face from corner electrode ‘b’ to the diagonally opposite electrode. (b) XY plot for a timing gate of 280ns.

$$\equiv \quad t_{disc}(\Delta E_{Gas}) - t_{disc}(p) \tag{7}$$

where $t_{disc}(\Delta E_{Gas})$ is the time taken for the Gas energy signal to rise above its MA discriminator level. The data here are from the COINC experiment and so there is only TDC data for the fastest position signal. If it is assumed that the position dependence of $t_{disc}(\Delta E_{Gas})$ is negligible, then for events with $\Delta E_{Gas} >$5MeV,

$$t_{gp} \approx c - t_{disc}(p) \tag{8}$$

where c is a constant. From the PSD model it was found that for particles incident near the PSD corner the value of $t_{disc}(p) \rightarrow 0$. At the PSD corners $t_{gp} \approx c =$ 4ns, therefore ignoring this small 4ns offset, $t_{gp} = t_{disc}(p)$. A plot of t_{gp} against X for a 2mm wide, corner–to–corner slice of data across the face of a PSD is shown in figure 7. The majority of the data corresponds to elastically scattered $\sim$ 170MeV ^{24}Mg ions. It can be seen that $t_{disc}(p) > t_{disc}(\Delta E_{Gas})$, with $t_{disc}(p) \leq$350ns.

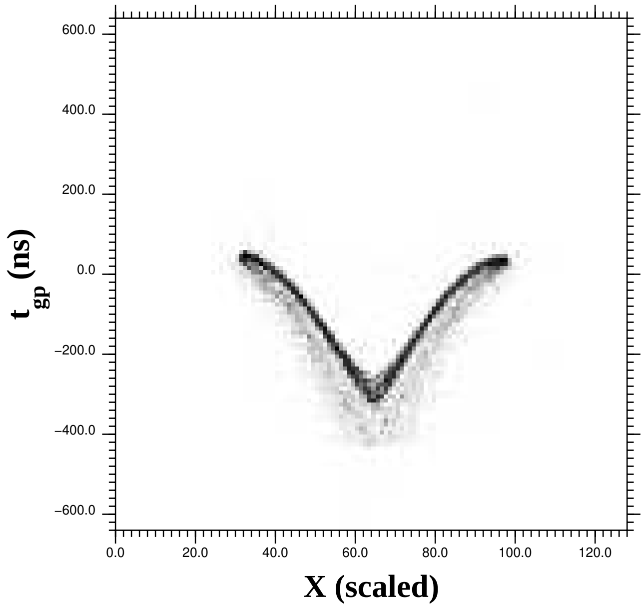

Figure 7: Plot of t_{gp} against X for a central 2mm wide slice of data across the face of a PSD.

Although the time–walk for the slower position signals was not measured it is safe to assume they show a similar trend to figure 6(a), with the slowest signals up to 3.5 times slower than those emanating from the detector centre. This means that the slowest position signals in the data shown in figure 7 could fall up to 1μs behind the Gas signal even for 170MeV events!

4 α–Particle Tests with New Data Acquisition

4.1 Background

Eight Hamamatsu PSDs were mounted in the central MEGHA module. Tests were made using an α–particle source (^{241}Am) to ascertain the effect of the new DA on the PSD performance.

These PSDs were used previously by CDF/GD in December 1996. Their leakage current history is summarised table 1, and gives a good indication of the damage sustained. Although the leakages currents listed are not severe, the position spectra displayed an effect which was attributed to radiation damage. This effect can be seen in figure 8(b) – " ... Low count halo around central cluster. High count clustering at edges of detector. These effects were observed in elastics and ^{12}C – ^{12}C gated coincidences from reaction data [6]". The XY spectrum from the same PSD taken earlier in the December 1996 experiment is shown in figure 8(a) for comparison.

PSD	9/12/96	start	end
1	0.6	0.2	0.3
2	1.5	0.5	0.7
3	0.4	0.25	0.35
4	1.6	0.55	0.75
5	1.6	0.5	0.8
6	0.5	0.1	0.2
7	1.6	0.6	0.85
8	0.6	0.05	0.15

Table 1: Leakage current history of PSDs. Currents are all measured in μA . 9/12/96 is the end of the CDF/GD experiment. 'start' and 'end' refer to the current α–particle testing.

This same effect was seen in the data of SPGC/CAB in January 1998, with PSDs mounted in the strip array. In addition to this effect, at low energies, the position information appeared to be severely corrupted. The only similarity between the PSD instrumentation for the two runs was in the choice of main amplifiers; both experiments used the new style of computer controlled MEGHA MA – this gives the first pointer as to where the problem may lie.

(a) (b)

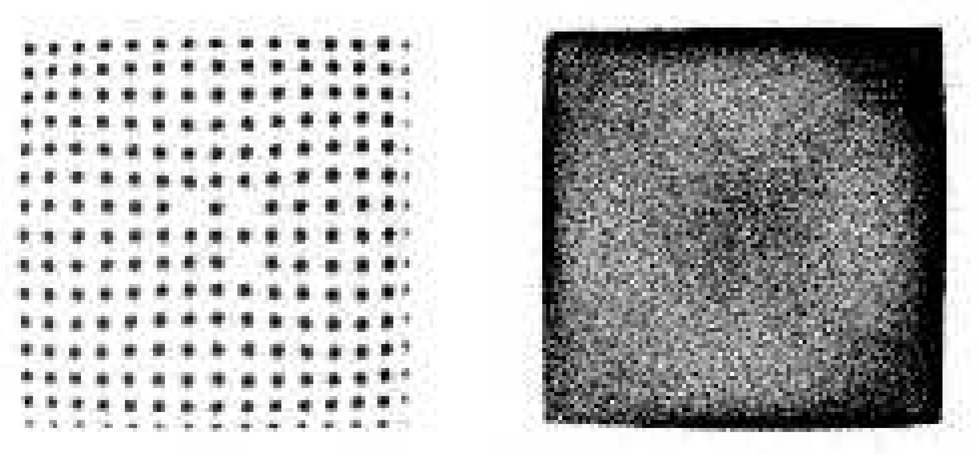

Figure 8: Typical XY spectrum for the December 1996 experiment (175MeV ^{28}Si + ^{197}Au . (a) Start of experiment – no halo effect, (b) near the end of the experiment – halo clearly seen.

4.2 Experimental Set–up

The ^{241}Am α–particle source was placed on the new downstream target ladder. To check for possible position distortions the calibration grid[7] was fixed to the module window frame. There were no mylar windows on the module. The chamber pressure was kept between $10^{-2} \rightarrow 10^{-3}$torr throughout the experiment. The PSDs were each biased to 100V.

The position signals were shaped to 2μs in un–modified MEGHA MAs. In four separate runs the energy signals were shaped to 2 and 10μs in both the un–modified and Dave–Smith–modified MEGHA MAs. The DA was configured to trigger off any signal. The discriminator levels were set just in the noise for the position MAs, and above the noise for the energy MAs.

4.3 Results

Figures 9(a) and (b) show the position spectra for PSDs 1 and 5. The PSDs with higher leakage currents (2,5,7[8]) showed the 'halo' of low count density, whereas those

[7]The calibration grid consisted of eight sets of 17×17 holes of 1mm diameter spaced at 3mm, each aligned to a telescope. Scattering of the α's from the hole edges combined with the large grid–to–PSD distance (50mm) and poor intrinsic position resolution at low energies ($\sim$ 2mm @ 5MeV) washed out the grid image in the position spectra.

[8]Position signal 'd' was missing for PSD 4.

with lower leakage currents (1,3,6,8) did not. It was shown in sections 2 and 3 that large discrepancies in the timing of the PSD signals at low energy leads to a variety of low energy thresholds (figures 2, 4 and 6(b)). However, the halo effect does not fit any of these predictions. Furthermore, the effect is energy independent and has been seen at $\sim$ 35MeV by SPGC/CAB and at $\sim$ 175MeV (see figure 8(b)), suggesting a different mechanism is responsible.

In figure 10 the variation in the timing difference between the diagonally opposite position signals 'a' and 'd' (t_{ad}) is plotted as a function of X for a corner 'a' to corner 'd' slice of data across the face of PSD 2. The spectrum in the background shows the count density for this slice. Dips in the count density due to the halo structure appear at $\pm$10mm, and correspond to the positions of the minima and maxima of t_{ad}.

The maximum values of t_{ad} and the energy signal ballistic deficit (B_D) are plotted as a function of leakage current in figure 11. Both parameters are strongly correlated with leakage current, or equivalently the integrated radiation exposure of the PSD. The ballistic deficit is related to t_{ad}, or more generally, the timing of all the PSD signals, and is caused by the undershaping of the slower preamplifier (PA) signals in their MA. The slow rise–time signals trigger the MA threshold pulse late – leading to poor timing – have a larger ballistic deficit, and the peak of the unipolar output of the MA is slightly delayed and broadened. The ballistic deficit and the width of the unipolar peak are independent of energy.

The un–modified MAs have been shown to have problems peak–detecting longer unipolar pulses. If the probability of NOT detecting a peak is proportional to the width of the peak, then the probability is also related to the rise–time of the PA pulse (independent of the particle energy) and hence any of the timing measurements (eg. t_{ad}). Thus the count density is expected to follow the trend of t_{ad} (for mono–energetic particles) as in figure 10, be independent of energy (as seen in a comparison of figures 8(b) and 9(b)), and show worse halo effects for the more heavily radiation damaged PSDs – since the PA rise–times are approximately proportional to the leakage current, as in figure 11.

The effect of not detecting the peak properly can be illustrated by looking at the energy signals shaped to 10μs in the un–modified MAs. Figure 12(a) shows the energy spectrum for PSD 5. The peak labelled A corresponds events in which the peak has been detected correctly to give the full pulse height. Events in region B are those for which the peak has not been detected properly to give approximately half the true pulse height. The XY spectrum for those events in peak A is plotted in figure 12(b). Only the quickest rise–time signals, emanating from the PSD corners and edges, are recorded at full pulse height. The distribution of events in figure 12(b) should be compared to that in figure 9(b); the ring of events form the outside of the

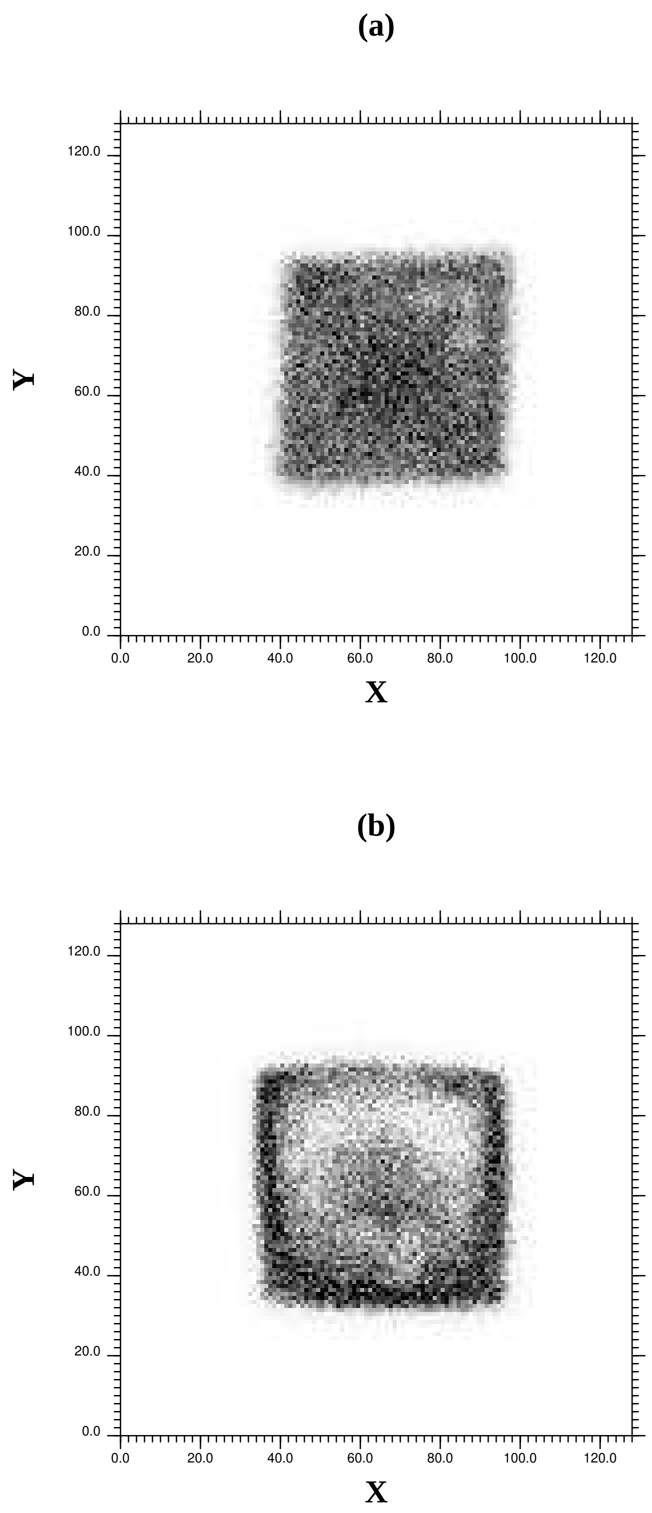

Figure 9: XY spectra for (a) PSD 1 and (b) PSD 5.

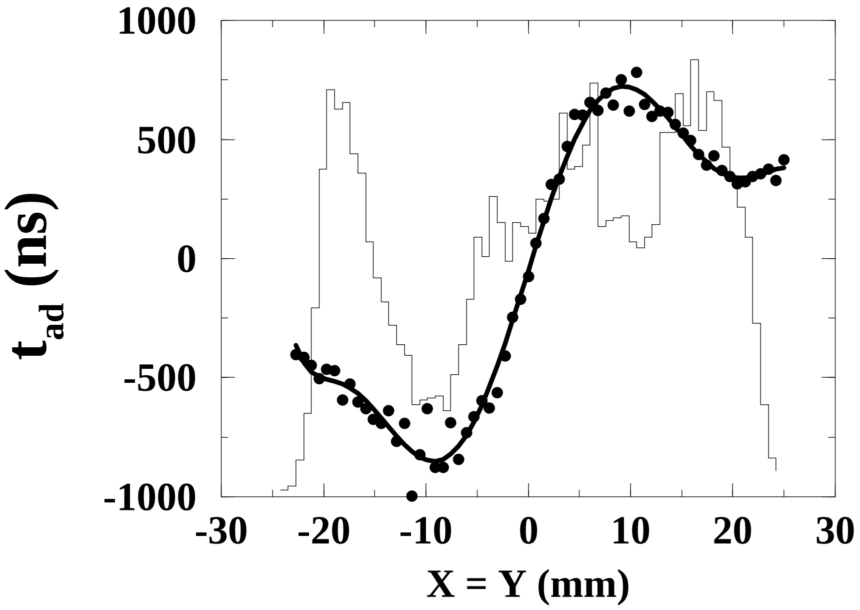

Figure 10: t_{ad} as a function of X from corner 'a' to corner 'd'. The bold line is an 8^{th} degree polynomial fit to the data. The spectrum in the background shows the count density for the slice of data.

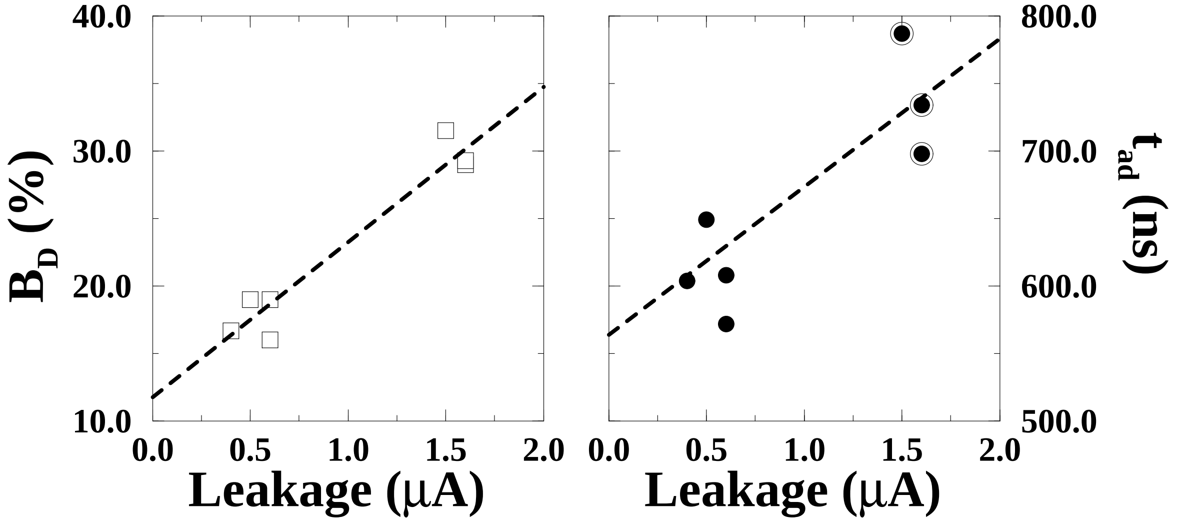

Figure 11: Ballistic deficit and t_{ad} as a function of leakage current. The circled data points correspond to detectors exhibiting the halo effect.

halo.

For the un–detected position signals from the α–particle data the recorded pulse height would be pushed below threshold. The number of events with a single position

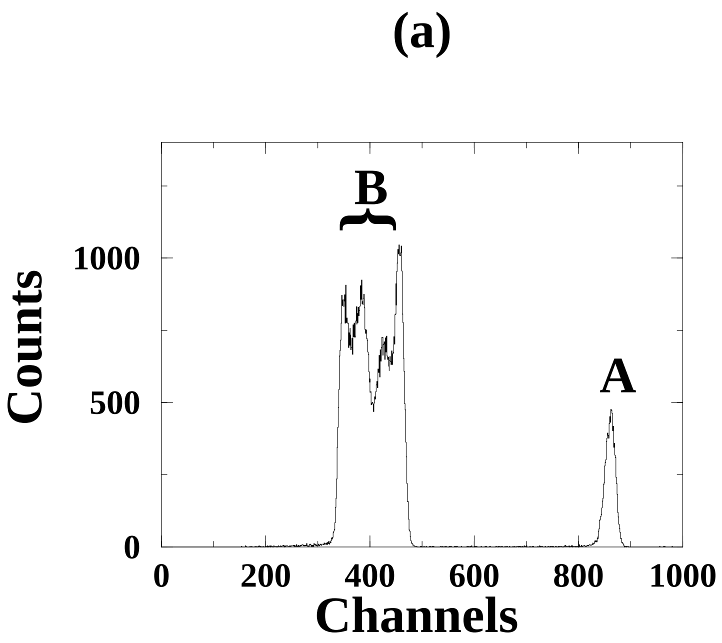

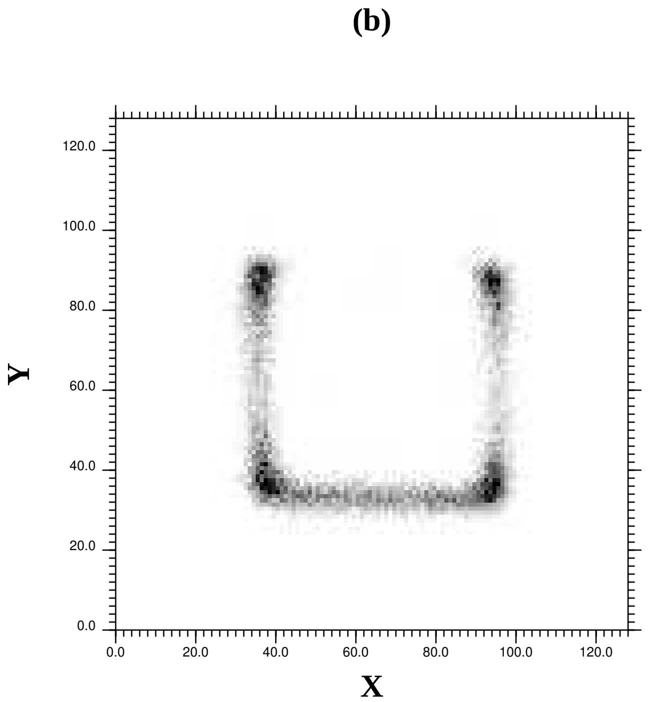

Figure 12: (a) Energy spectrum for PSD 5 for a shaping time of 10μs in an un-modified MEGHA MA. (b) XY spectrum for events in peak A.

signal below threshold are listed in table 2 as a percentage of the total number of events with at least three position signals and an energy signal. The majority of the data has at least one position signal below threshold, yet the α's should have been of sufficient energy to overcome the low energy detection threshold – this suggests the peak detect fault is to blame.

Missing signal	% of events
d	12.4
c	24.5
b	12.3
a	7.2

Table 2: Missing position signals from PSD 2 as a percentage of the total number of events with at least three position signals and an energy signal.

For higher energy data, such as that of SPGC/CAB, the position signals missing the peak detect would still fall above the detection threshold, but the position information would be destroyed. Attempts to reconstruct the event would yield a severely distorted position spectrum, as was the case.

5 Solutions

Further tests are needed. The first would be to shape all PSD signals using Dave–Smith–modified MEGHA MAs. These have been shown to correctly detect energy signals shaped to $10\mu s$.

The predictions of the low energy thresholds due to the timing constraints on the WALK signals made in section 3 seem to be a little excessive. From figure 10 it is clear that the PSD signal timing is within $1.6\mu s$ even for 5MeV α–particles. However, there may be problems at this energy if a coincidence requirement is made between the position signals in the MALUs. The effect of demanding a Gas signal coincidence also needs to be investigated.

References

[1] B.J. Varley, Computer Software 'GLADYS', University of Manchester, unpublished.

[2] R.L. Cowin and D.L. Watson, Nucl. Instr. Meth. A399(1997)365–381 and CHARISSA preprint CH/prep/97/02

[3] R.L. Cowin, CHARISSA technical report CH/Tech/96/02

[4] R.L. Cowin, Ph.D. Thesis, University of York 1997, unpublished.

[5] M. Bruno, M. D'Agostino, M. Fiandri, E. Fuschini, P. Milazzo, S. Ostuni, F. Gramegna, I. Iori, L. Manduci, A. Moroni, R. Scardaoni, P. Buttazzo, G. Margagliotti and G. Vannini, Nucl. Instr. and Meth. A311(1992)189–194

[6] C.D. Freeman, private communication.